Journal of Physiology (1996), **490.1**, *pp.*129–147

Electrophysiological and morphological properties of interneurones in the rat dorsal lateral geniculate nucleus *in vitro*

Stephen R. Williams, Jonathan P. Turner, Caroline M. Anderson and Vincenzo Crunelli

Department of Physiology, University of Wales Cardiff, Museum Avenue, Cardiff CF1 1SS, UK

1. Intracellular recordings were made from putative interneurones ($n = 24$) and thalamocortical (TC) projection neurones ($n = 45$) in slice preparations of the rat dorsal lateral geniculate nucleus (dLGN) in order to compare the electrophysiological properties of these neuronal types.

2. Intracellular injection of biocytin to electrophysiologically identified neurones ($n = 34$) revealed the morphology of putative interneurones ($n = 4$) to be similar to class B and that of TC neurones ($n = 30$) to be similar to class A Golgi-impregnated neurones.

3. Interneurones had resting membrane potentials (−52 mV) relatively positive to those of TC neurones (−63 mV), shorter time constants (36·8 and 58·2 ms, respectively), but similar steady-state input resistances (164 and 180 MΩ, respectively). Steady-state voltage–current relationships were nearly linear in interneurones, but highly non-linear in TC neurones.

4. The structure of action potential firing evoked at the break of hyperpolarizing voltage transients was dependent upon neuronal type. Interneurones fired a single action potential or a burst of action potentials with a maximum frequency of <130 Hz, whilst TC neurones fired a high frequency burst with a minimum frequency of >250 Hz. In addition, well-defined burst firing of action potentials in response to depolarizing voltage excursions, from membrane potentials negative to −65 mV, could be evoked in TC neurones, but not in interneurones.

5. The directly evoked action potentials of interneurones were characterized by an initial slow pre-potential preceding the fast upstroke of the action potential. The amplitude and width of interneurones' action potentials were smaller than those of TC neurones and the amplitude and duration of the single action potential after-hyperpolarization were greater in interneurones. Both interneurones and TC neurones fired action potentials repetitively in response to suprathreshold voltage excursions, with interneurones demonstrating a greater degree of spike-frequency adaptation. Following a train of action potentials, interneurones and TC neurones generated a slow after-hyperpolarizing potential: in interneurones but not TC neurones this potential was followed by a slow depolarizing potential.

6. An intrinsic, subthreshold membrane potential oscillatory activity with a mean frequency of ~8 Hz was observed in interneurones.

7. Electrical stimulation of the optic tract evoked in interneurones apparently pure EPSPs, pure IPSPs or a mixture of EPSPs and IPSPs. EPSPs were found to be biphasic and mediated by the activation of non-*N*-methyl-D-aspartate (NMDA) and NMDA excitatory amino acid receptors. IPSPs and the response to the iontophoretic application of GABA were found to reverse between −65 and −70 mV. The application of $GABA_B$ receptor agonists failed to affect the membrane properties of six of seven interneurones tested. In addition spontaneous EPSPs and IPSPs were recorded in interneurones.

8. These results demonstrate that the electrophysiological properties of putative interneurones are distinct from those of TC neurones of the rat dLGN. The implications of these findings for the control of visual responsiveness of TC neurones are discussed.

The receptive field properties of thalamocortical (TC) projection neurones of the dorsal lateral geniculate nucleus (dLGN) and the transfer ratio of retinal input to TC neurone output is known to be modulated by inhibitory processes (Sillito & Kemp, 1983; Berardi & Morrone, 1984; Heggelund & Hartveit, 1990; Norton & Godwin, 1992). The basis of such inhibition is thought to be the generation of GABA-mediated inhibitory postsynaptic potentials (IPSPs) evoked in a feed-forward manner through the activation of dLGN interneurones (Lindstrom, 1982; Crunelli, Haby, Jassik-Gerschenfeld, Leresche & Pirchio 1988; Soltesz, Lightowler, Leresche & Crunelli, 1989) and in a feed-back manner through peri-geniculate nucleus (PGN) neurones (Hale, Sefton, Baur & Cottee, 1982; Lindstrom, 1982), driven by the output of TC neurones (Ahlsen & Lindstrom, 1982). However, the precise contribution of these sources to the inhibition of TC neurones is poorly understood (but see Jones & Sillito (1994) for the involvement of the PGN).

The direct retinal input to interneurones (Hamos, Van Horn, Raczkowski, Uhlrich & Sherman, 1985; Humphrey & Weller, 1988), the monosynaptic axonal output connections of interneurones to sites proximal to the soma of TC neurones (Montero, 1987) and the possible involvement of dendro-dendritic inhibition provided by interneurones (Hamos *et al.* 1985) suggest that interneurones are ideally placed for the modulation of geniculo-cortical information transfer. Indeed in the rat and cat dLGN, IPSPs evoked by interneurones have been shown to inhibit the generation of action potentials in TC neurones (Crunelli *et al.* 1988; Soltesz *et al.* 1989). Although data are available concerning the membrane properties of cat dLGN interneurones (McCormick & Pape, 1988) and dissociated rat interneurones (Pape, Budd, Mager & Kisvardy, 1994), little is known about the mode and pattern of action potential generation, the nature of the excitatory input to, or the presence and nature of the inhibition of, these neurones. These data are critically important in an examination of the role of interneurones in the modulation of the pattern of TC neurone output.

Using an *in vitro* preparation of the rat dLGN, we report that interneurones may be electrophysiologically and anatomically identified following intracellular injection of biocytin. The membrane properties, firing pattern and synaptic responsiveness of interneurones revealed by these experiments suggest a new level of physiological complexity within the circuitry of the dLGN. Preliminary reports of some of the results presented here have been published (Williams, Turner & Crunelli, 1994; Williams, Anderson & Crunelli, 1995*a*).

METHODS

Slicing and recording procedures

The preparation and maintenance of brain slices of the rat dLGN were similar to those described previously (Crunelli, Kelly, Leresche & Pirchio, 1987). Male Wistar rats (150–200 g) were decapitated and a block of tissue containing the dLGN was separated from the rest of the brain by two cuts made parallel to the plane of the optic tract. The tissue block was stuck to the stage of a Vibroslice (Campden Instruments), bathed in a continuously aerated (95% O_2, 5% CO_2) cold (< 1 °C) medium containing (mM): NaCl, 134; $NaHCO_3$, 16; KCl, 5; KH_2PO_4, 1·25; $MgSO_4$, 5; $CaCl_2$, 2; and glucose, 10; and were sliced at a thickness of 400–500 μm. The slices were transferred to a storage bath, submerged in the same medium at room temperature, where they remained viable for transfer to the recording chamber. A single brain slice was then transferred to the recording chamber of an interface-type bath, and perfused with the same medium, warmed to a temperature of 35 ± 1 °C, for at least 30 min. Thirty minutes before recording commenced the perfusion medium was replaced with one of similar composition, but containing 2 mM KCl and 1 mM $MgSO_4$.

Intracellular sharp electrode recordings were made with glass microelecetrodes (GC 120F, Clark Electromedical Instruments, Pangbourne, Reading, UK) filled with 1 M potassium acetate or 2% biocytin dissolved in 1 M potassium acetate (resistance, 80–120 MΩ). Potentials were recorded with an Axoclamp-2A amplifier (Axon Instruments), configured in bridge-balance mode, and stored on a Biologic DAT recorder (Intracel, Royston, Herts, UK). Data were subsequently filtered (DC to 1–30 kHz) and digitally sampled. Results were analysed with a microcomputer running pCLAMP software (Axon Instruments). Postsynaptic potentials were evoked with the use of a bipolar tungsten electrode placed amongst, and parallel to, the fibres of the optic tract. Using low frequency (0·05–0·1 Hz) electrical stimulation (20–50 μs, 1–20 V) excitatory postsynaptic potentials (EPSPs) and/or IPSPs were generated in approximately 50% of TC neurones tested. Numerical results are expressed in the text as means ± S.E.M. and statistical significance was tested ($\alpha = 5\%$) using Student's t test.

An independently mounted, multibarrelled micropipette (4–6 μm tip diameter) was used to eject iontophoretically GABA (1 M, pH 5), while a barrel containing 1 M NaCl was used for automatic current balancing. Retaining current was applied to the GABA-containing barrel when necessary. All other drugs were dissolved in and applied via the perfusion medium. Drugs were obtained from the following sources: 6-cyano-7-nitroquinoxaline-2,3-dione (CNQX) and DL-2-amino-5-phosphonovaleric acid (DL-AP5), Tocris Cookson, Bristol, UK; GABA, (±)-baclofen and γ-hydroxy-butyric acid, Sigma; 1-(4-amino-phenyl)-4-methyl-7,8-methylene-dioxy-5H-2,3-benzodiazepine (GYKI 52466) was kindly donated by Dr Istvan Tarnawa, Institute for Drug Research, Budapest, Hungary.

Dye injection and anatomical procedures

Intracellular dye-filling of neurones with biocytin was accomplished without the need of an ejection protocol, since preliminary experiments had shown that recordings of duration greater than 10 min allowed the subsequent recovery of well-filled neurones. When using biocytin-filled electrodes, we typically recorded from a maximum of three neurones in each slice and the approximate location of neurones was marked on drawings of brain slices. At the end of recording, the brain slice was maintained for at least 1 h, before transfer to a fixative solution (4% paraformaldehyde in 0·1 M phosphate-buffered saline (PBS), pH 7·4). Slices were maintained in the fixative for 8–14 h and then transferred to 0·1 M PBS, embedded in agar and re-sectioned at 50 μm. To quench background peroxidase activity and permeabilize the tissue, sections were incubated with 0·3% H_2O_2 in PBS with 0·4% Triton X-100 (Sigma) for 30 min, rinsed to clear the H_2O_2 and then incubated for a further 2 h with an

avidin–biotin–horseradish peroxidase complex (Elite ABC kit, Vector Labs, Peterborough, UK) in 0·4% Triton X-100 PBS. This step was followed by a 5–10 min wash in 1% cobalt chloride (BDH, Lutterworth, UK) in 0·02 M Tris buffer (Sigma), in order to intensify the subsequent reaction and produce a blue/black product. To visualize the filled neurones, sections were reacted with 0·1 M diaminobenzidine tetrahydrochloride (Sigma) in 0·1 M Tris buffer (pH 7·2 at 25 °C) and 0·02% H_2O_2. Sections were then rinsed in PBS and arranged on slides using a gelatine mounting solution. After air-drying the mounted sections were dehydrated in 10% incremental concentrations of alcohol (50–100%), defatted in xylene and mounted in DPX (Aldrich, Gillingham, UK).

The morphology of neurones was examined using a light microscope and measurements of somal and dendritic area were made from camera lucida reconstructions made at ×1300 and ×200, respectively. Somal and dendritic areas were calculated according to the methods of Spreafico, Schmechel & Rustioni (1983) where the area (A) is calculated from the formula $A = \pi ab$, where a and b are the minimum and maximum somal/dendritic radii. This method assumes the somal/dendritic fields to be elliptical when a and b are different or more circular as a approaches b. Final, illustrated camera lucida reconstructions were made at a magnification of ×625 or ×800. Measurements were not corrected for tissue shrinkage.

RESULTS

Previous morphological evidence has indicated that neurones of the rat dLGN may be divided into two groups termed class A and B (Grossman, Liberman & Webster, 1973; Gabbot, Somogyi, Stewart & Hamori, 1986). Class B neurones are known to be both GABA positive and express glutamic acid decarboxylase immunoreactivity and so have been suggested to be local circuit inhibitory interneurones (Ohara, Liberman, Hunt & Wu, 1983; Gabbot *et al.* 1986), whilst class A neurones are suggested to be TC neurones (Grossman *et al.* 1973; Ohara *et al.* 1983; Gabbot *et al.* 1986). During the course of our evolving study of the electrophysiological properties of rat dLGN neurones we have recorded two populations of neurones, with distinct electrophysiological properties. A previous study utilizing combined electrophysiological and morphological analysis (Crunelli *et al.* 1987) has described the properties of rat dLGN neurones that were morphologically similar to class A neurones and exhibited electrophysiological properties similar to morphologically identified TC neurones from the thalamus of other species (Jahnsen & Llinás, 1984; McCormick & Pape, 1988). Isolated recordings of presumed interneurones of the rat dLGN (Leresche, Lightowler, Soltesz, Jassik-Gershenfeld & Crunelli, 1991) have indicated that their membrane properties are similar to those of morphologically identified interneurones of the cat dLGN (McCormick & Pape, 1988). We utilized the classification system of McCormick & Pape (1988) to identify interneurones, and from our observations have extended it to produce a set of criteria that allowed the differentiation between the electrophysiological properties of interneurones and TC neurones. The distinguishing properties were: (i) the shape of steady-state voltage–current relationships, (ii) the shape of single action potentials and their fast after-hyperpolarizing potentials, (iii) the pattern of tonic action potential firing, (iv) the presence of a post-train slow after-depolarizing potential, (v) the structure and frequency of action potential firing evoked at the break of hyperpolarizing voltage excursions and (vi) the presence of ~8 Hz subthreshold oscillatory activity. These criteria together with correlated morphological analysis have allowed us to identify unambiguously interneurones and TC neurones. The three neurones that appeared to have electrophysiological properties transitional between these two groups were excluded from our analysis. Our results, therefore, describe the comparative electrophysiological and morphological properties of interneurones and TC neurones; their distinct properties are described below and summarized in Fig. 1.

The experiments described in this paper are based on recordings made from sixty-nine neurones: of these twenty-four were physiologically classified as putative interneurones and forty-five as putative TC neurones. These figures do not faithfully reflect the ratio of TC neurone to interneurone recorded, as putative interneurones were collected during our evolving studies of rat dLGN neurones recorded under identical conditions to those reported here. The results obtained from the other TC neurones of this data base have appeared elsewhere (Turner, Leresche, Guyon, Soltesz & Crunelli, 1994; Williams, Turner & Crunelli, 1995). Taken together, the percentage of putative interneurones of the total number of rat dLGN neurones reported is 16%.

Morphological properties

The intracellular injection of biocytin allowed the examination of neuronal morphology, in thirty-four well-filled of forty injected neurones. Of these, four were classified as putative interneurones and thirty as presumed TC neurones by their morphological properties (Grossman, Liberman & Webster, 1973). Occasionally putative interneurones and TC neurones were recorded from the same slice preparation (Fig. 1), allowing a direct comparison between neurones of the same animal. Putative interneurones had small fusiform somata with a mean area of $170{\cdot}2 \pm 15{\cdot}7\ \mu m^2$ ($n = 4$). Each neurone had two principle dendrites originating from opposite poles of the soma, so that the neurones had a bipolar shape that was oriented in the dorso-ventral plane (Figs 1 and 2). In one case, two additional lower calibre primary dendrites emerged from the cell body, although the low calibre of these dendrites did not detract from the predominant bipolar appearance of the neurone. Primary dendrites branched dichotomously; these and higher order dendrites possessed short formations that terminated in grape-like structures (Figs 1 and 2). Primary and daughter dendritic branches gave rise to fine calibre, varicose branches that bifurcated and often ended in beaded formations (Figs 1 and 2). The total dendritic field area was $0{\cdot}129 \pm 0{\cdot}027\ mm^2$; however, since the secondary dendrites of an interneurone (Fig. 2) exited from the tissue

sections, this parameter underestimates the total dendritic field area. We were not able to identify unambiguously the axons of putative interneurones: since some dendrites exhibited an axon-like appearance, it may be possible that such neurites represent the axonal projections of interneurones. Although one injection of biocytin to a presumed interneurone failed to reveal its full morphology, we were able to visualize a primary dendritic tree that was similar to those of the other interneurones (not illustrated).

Presumed TC neurones were found to have more spherical somata (Figs 1 and 2), with an average area of $270{\cdot}9 \pm 12{\cdot}0\ \mu m^2$ ($n = 30$), which was significantly greater than that of putative interneurones ($P < 0{\cdot}05$, $T = 2{\cdot}97$). A variable number of primary dendrites (3 to 10; mean = 6·0), which typically branched dichotomously, emerged from somata and gave rise to daughter dendrites that further branched to form 2nd to 7th order terminal dendrites (mean = 5, $n = 88$). The calibre of terminal dendrites did not appreciably differ from those of secondary dendrites. In all cases dendrites were radially oriented, with a mean dendritic area of $0{\cdot}101 \pm 0{\cdot}07\ mm^2$ ($n = 30$). The primary dendrites of presumed TC neurones did not carry any specializations, while the secondary and higher order branches possessed stud-like appendages or spines (Figs 1 and 2). Presumed axons, identified by their low calibre and branchless appearance, were filled in ~50% of TC neurones (Figs 1 and 2). The course of the axons could be traced for some neurones; the axons were found to project towards the dorso-medial quadrant of the brain slice, where the nucleus reticularis thalami (NRT) would be located if included in the brain slice. We were not able to identify axonal branching or terminal arborization of axons within the dLGN.

The electrophysiological properties of the neurones that were not filled with biocytin were found to be similar to those of filled interneurones or TC neurones, indicating that these electrophysiological features represent an unequivocal method for the identification of interneurones and TC neurones. We have, therefore, omitted the prefix

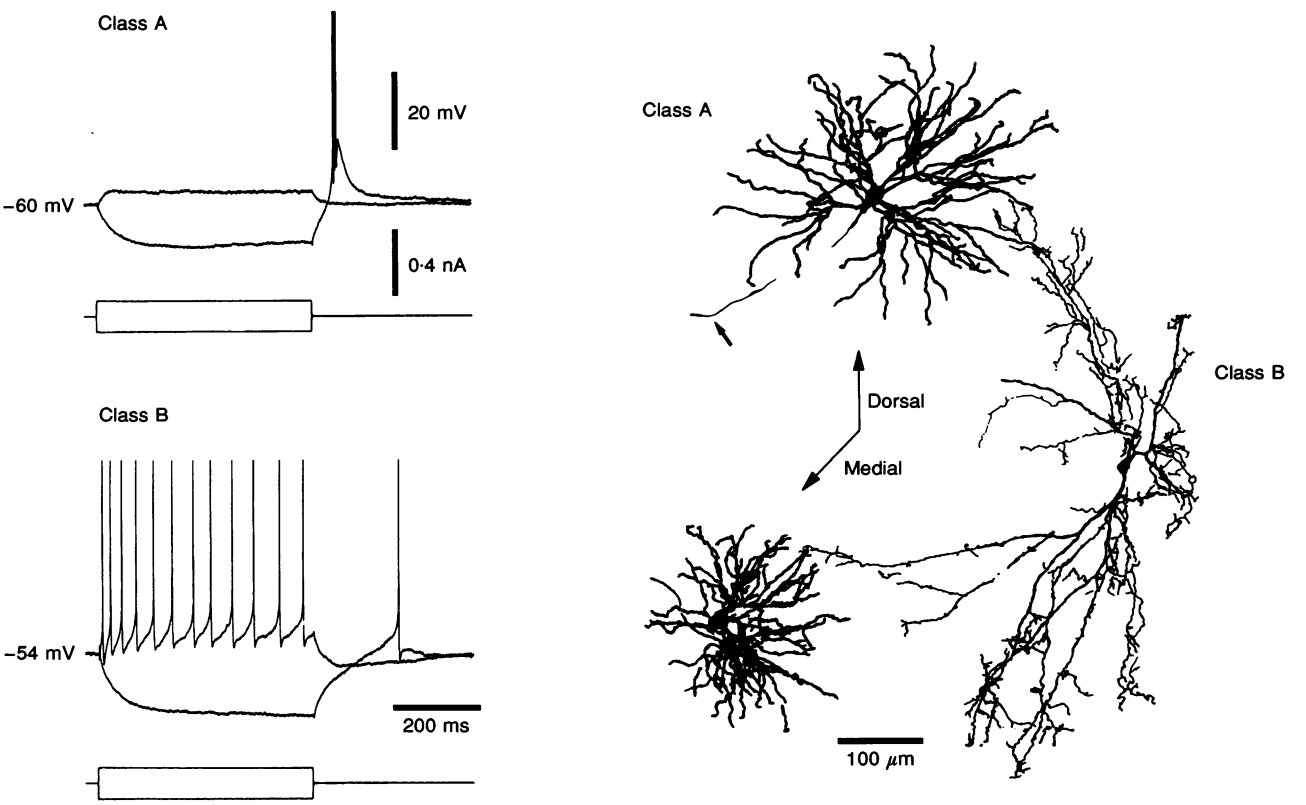

Figure 1. Electrophysiological and morphological features of an interneurone and two TC neurones recorded from the same slice preparation

Intracellular voltage records from a class A TC neurone demonstrates the resting potential, the rectification properties and the high frequency rebound firing driven by a low threshold Ca^{2+} potential, typical of this class of neurone. In comparison, the recording of a class B interneurone indicates the relatively positive resting potential, the minimal rectification and the weak rebound firing driven by a small amplitude, transient depolarizing potential. Traces beneath voltage records represent current injection. The morphology of these neurones is shown in camera lucida reconstructions (× 625). The small oblique arrow indicates the point where the axonal projection turns towards the NRT. In voltage records action potential amplitude has been truncated for clarity.

presumed or putative from a description of neurones throughout the remaining sections of the paper.

Membrane properties

The resting potential of interneurones (−52 ± 1 mV, $n = 24$) was found to be significantly ($P < 0{\cdot}05$, $T = 9{\cdot}09$) more positive than that of TC neurones (−63 ± 1 mV, $n = 30$). Of our sample, 13% of interneurones were found to fire action potentials spontaneously, when no current was injected through the recording electrode. The input resistance of interneurones (164 ± 15 MΩ, $n = 13$), calculated by taking the maximal slope of steady-state voltage–current relationships, was not significantly different ($P > 0{\cdot}05$, $T = 0{\cdot}74$) from that of TC neurones (180 ± 15 MΩ, $n = 19$). The shape of these relationships was, however, found to differ between the two groups (Fig. 2): interneurones demonstrated relatively linear voltage–current relationships, whilst those of TC neurones exhibited prominent rectification in both the depolarized and hyperpolarized direction. However, in 21% of interneurones a depolarizing sag was apparent during the course of large amplitude hyperpolarizing (>25 mV) voltage excursions; the degree of this time-dependent rectification was, in all cases, not as great as that for TC neurones (Fig. 2*A* and *C*). The construction of voltage–current relationships in interneurones at holding potentials separated by 10 mV, achieved by tonic injection of current through the recording electrode, indicated the presence of steady rectification. These procedures yielded a decrease in input resistance of 33 ± 10 MΩ per 10 mV negative shift in the holding potential ($n = 3$). The time constant of interneurones (36·8 ± 3·8 ms, $n = 24$), calculated by the fitting of a mono-exponential function to small (<10 mV)

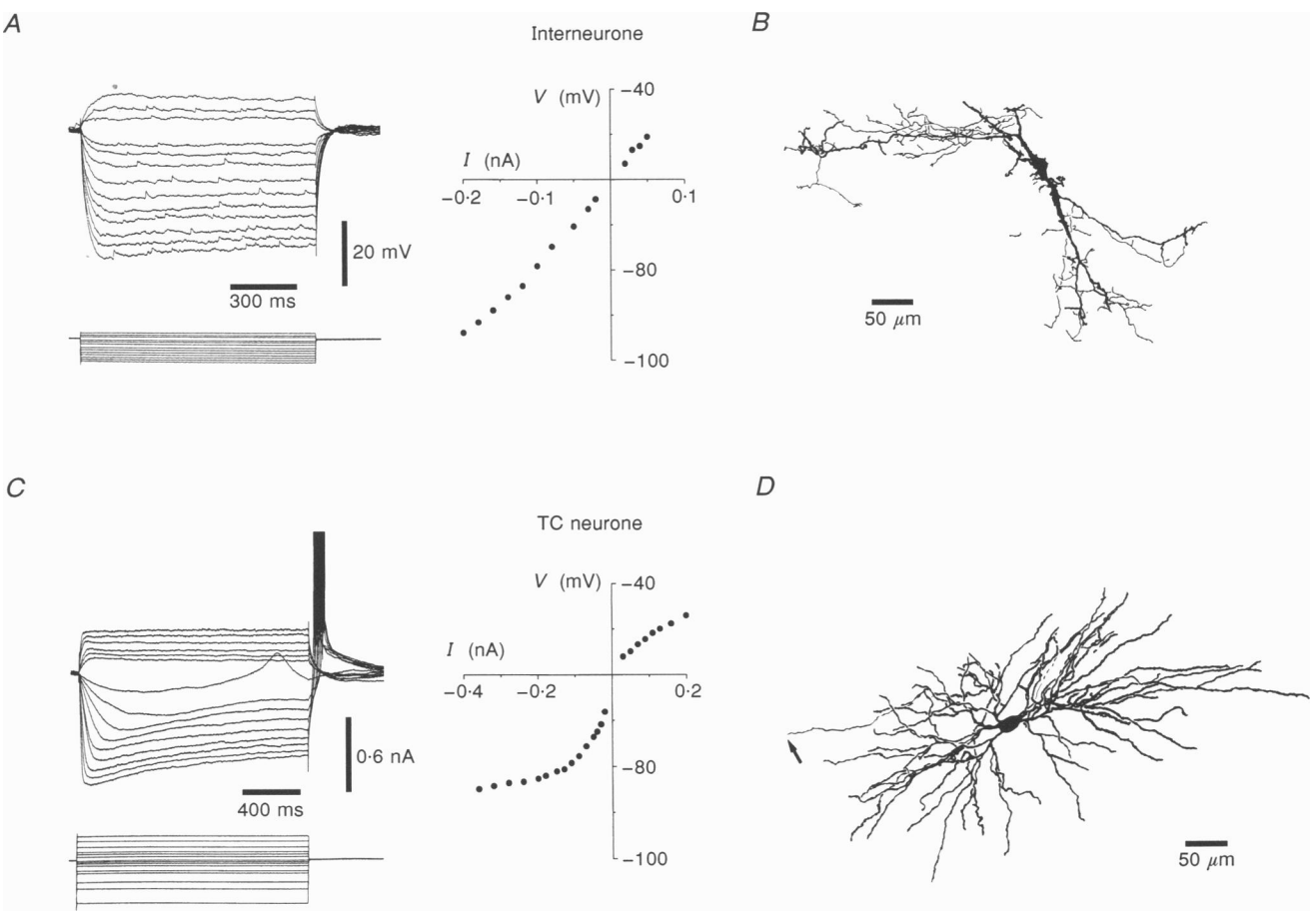

Figure 2. Voltage–current relationships of a morphologically identified interneurone and TC neurone

Families of voltage and current records (single traces) used for the construction of voltage–current relationships illustrated in the centre of the figure; the holding potential was set to −60 mV in both neurones by the tonic passage of current through the recording electrode. The shape of these relationships, measured at steady state for the interneurone (*A*) and the TC neurone (*C*) are clearly different, with the TC neurone exhibiting prominant rectification in the depolarized and hyperpolarized direction. The morphology of these neurones is shown in the camera lucida reconstructions (× 800) (*B* and *D*). The small oblique arrow in *D* indicates the axon of the TC neurone. The amplitude of action potentials has been truncated for clarity.

hyperpolarizing voltage excursions, was found to be significantly ($P < 0{\cdot}05$, $T = 2{\cdot}59$) shorter than that of TC neurones ($58{\cdot}2 \pm 6{\cdot}9$ ms, $n = 30$).

Single action potential properties

The properties of action potentials of interneurones and TC neurones were found to be different. Action potentials were evoked by the passage of positive current through the recording electrode for between 0·2 and 1·5 s; in each neurone action potentials of the greatest and smallest amplitude were measured. The amplitude of action potentials generated by TC neurones ($60{\cdot}5 \pm 1{\cdot}3$ mV, $n = 30$), when measured from firing threshold, was found to be significantly ($P < 0{\cdot}05$, $T = 3{\cdot}296$) greater than that of interneurones ($53{\cdot}6 \pm 1{\cdot}7$ mV, $n = 30$) (Fig. 3*A*). The duration of action potentials of TC neurones ($0{\cdot}54 \pm 0{\cdot}02$ ms, $n = 30$) was significantly ($P < 0{\cdot}05$, $T = 2{\cdot}356$) broader than those of interneurones ($0{\cdot}48 \pm 0{\cdot}02$, $n = 30$) when measured at half-height, but not when measured at their base ($1{\cdot}0 \pm 0{\cdot}03$, $n = 30$, and $0{\cdot}93 \pm 0{\cdot}04$, $n = 30$, respectively; $P > 0{\cdot}05$, $T = 1{\cdot}627$). The shape of the rising phase of the action potentials and the fast after-hyperpolarizing potential (fAHP) differed between the two groups. The fast rising phase of action potentials generated by interneurones was preceded by a slow ramp pre-potential (Fig. 3*B*) that was not present in TC neurones. Single action potentials were followed by a fAHP; the amplitude ($14{\cdot}95 \pm 0{\cdot}57$ mV, $n = 15$) and duration ($73{\cdot}83 \pm 9{\cdot}33$ ms, $n = 14$) of these potentials in interneurones were significantly greater ($P < 0{\cdot}05$, $T = 6{\cdot}231$, and $P < 0{\cdot}05$, $T = 3{\cdot}379$, respectively) than those of TC neurones ($10{\cdot}53 \pm 0{\cdot}42$ mV, $n = 15$ and $40{\cdot}27 \pm 3{\cdot}4$ ms, $n = 14$, respectively; Fig. 3*A* and *B*).

Repetitive firing properties

The action potential firing pattern of interneurones and TC neurones were found to be voltage dependent (Fig. 4*A* and *B*). In response to positive current steps imposed from holding potentials positive to −60 mV, both groups of neurones demonstrated a tonic firing pattern (Figs 4 and 5). Analysis of the structure of the firing pattern of interneurones revealed the presence of a slow and pronounced spike-frequency adaptation (Fig. 5*A*), while the spike-frequency adaptation of TC neurones (Fig. 5*B*)

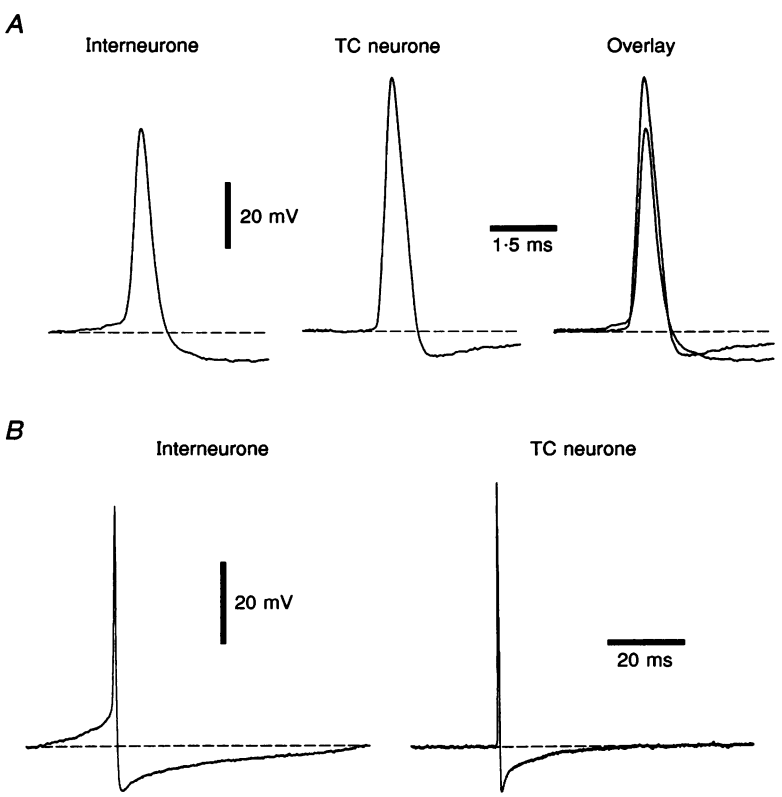

Figure 3. The shape, amplitude and after-hyperpolarization of single action potentials of interneurones are different from those of TC neurones

A, the amplitude and width of interneuronal action potential were found to be smaller than those of TC neurones. Action potential amplitude was measured from firing threshold and width at half-height. *B*, the amplitude and duration of interneuronal after-hyperpolarizing potentials were greater than those of TC neurones. The rising phase of interneuronal action potentials was characterized by a slow pre-potential (*B*), which is shown at a faster time base in *A*. Note that the records in *A* and *B* are drawn from different neurones.

occurred more rapidly, as indicated by plots of the instantaneous firing frequency against injected current (Fig. 5*A* and *B*). The kinetics of spike-frequency adaptation estimated from these relationships indicates that TC neurones have reached a steady state at the 5th interspike interval (ISI), whilst the firing frequency of interneurones is still adapting. As a percentage, the reduction in the firing frequency between the 1st and 5th ISI was 41 % for TC neurones ($n = 5$) compared with 21 % for interneurones ($n = 5$). The instantaneous firing frequency of interneurones and TC neurones at the 1st, 5th and 30th ISIs was found to be linearly related to the amplitude of the injected current (Fig. 5); at the 1st ISI, TC neurones responded at a frequency of 53·9 ± 12·2 Hz per 0·1 nA ($n = 5$), whilst interneurones fired with a frequency of 42·1 ± 8·4 Hz per 0·1 nA ($n = 5$). A considerable degree of variation was found in the firing frequency of TC neurones when measured at the first ISI (compare upper and lower graphs in Fig. 5*B*), a result that reflects a variation in the degree of rectification in the depolarized direction observed between TC neurones (not illustrated).

The firing patterns of interneurones and TC neurones were transformed when evoked from more negative holding potentials. The degree of spike-frequency adaptation of interneurones was found to be enhanced when action potentials were evoked from increasingly negative holding potentials (Fig. 4*A*). In TC neurones positive current steps imposed from holding potentials negative to −65 mV evoked a clear and isolated burst discharge that was imposed upon a transient depolarizing potential (Fig. 4*B*). Such transient depolarizing potentials have been described for TC neurones as low threshold Ca^{2+} potentials (Deschenes, Paradis, Roy & Steriade, 1984; Jahnsen & Llinás, 1984; Crunelli *et al.* 1987; Crunelli, Lightowler & Pollard, 1989). It is important to note that a well-defined burst of action potentials was not generated by interneurones in response to positive voltage excursions. The increased degree of spike-frequency adaptation when action potentials were evoked from holding potentials negative to −60 mV in interneurones suggests that a transient depolarizing potential evoked close to firing threshold may augment the firing frequency over the first few action potentials of a

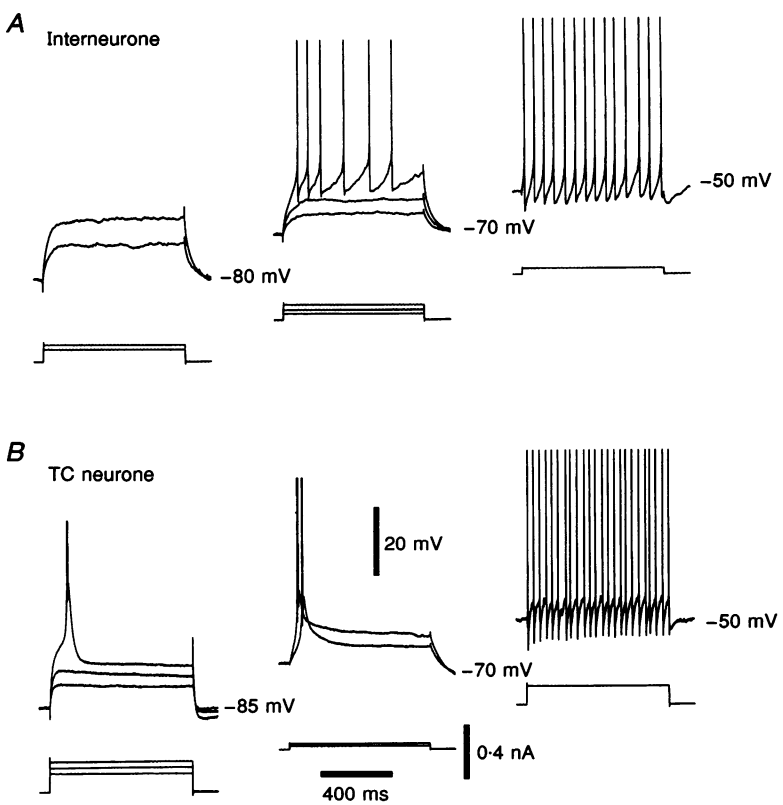

Figure 4. The pattern of action potential output is voltage dependent in TC neurones and interneurones

The action potential output evoked by injection of steps of positive current from holding potentials positive to −60 mV indicates that both neurones have the ability to generate action potentials repetitively. From potentials more negative than −65 mV, TC neurones (*B*), but not interneurones (*A*) were found to generate a burst discharge of action potentials that were isolated from any subsequent tonic firing. The degree of spike-frequency adaptation throughout the train of action potentials in interneurones was, however, found to be increased at more negative holding potentials (*A*). Note in the middle trace *A* the short delay to action potential firing. The amplitude of action potentials has been truncated for clarity.

train (Fig. 4*B*). These data, however, clearly illustrate that when action potentials are evoked from holding potentials positive to −60 mV, interneurones, but not TC neurones, exhibit a slow and pronounced spike-frequency adaptation.

Following a train of action potentials a slow after-hyperpolarizing potential (sAHP) was observed in both interneurones and TC neurones (Fig. 6). The amplitude of these potentials was found to be related to the number of action potentials generated during the train (Fig. 6). In

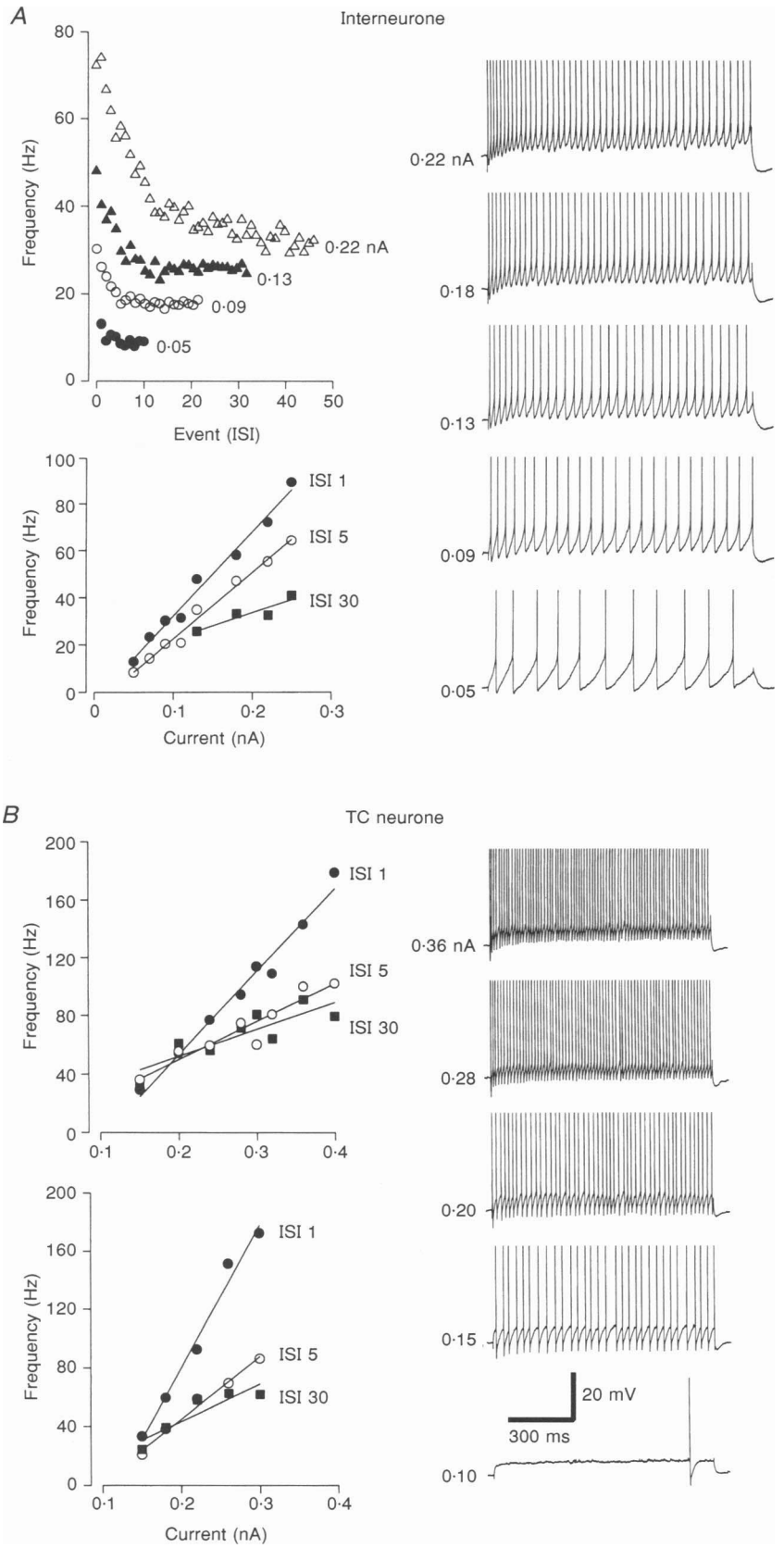

Figure 5. The patterns of spike-frequency adaptation are different between interneurones and TC neurones

A, the pattern of spike-frequency adaptation of a representative interneurone is shown from the voltage traces and the instantaneous frequency event graph; note the slow and pronounced adaptation pattern. The lower graph illustrates the linear relationship between the injected current and the instantaneous firing frequency measured at the 1st, 5th and 30th interspike interval (ISI). The current–discharge relationship was constructed from a holding potential of −54 mV. *B*, a representative TC neurone shows a pattern typified by fast spike-frequency adaptation over the first few action potentials of the train. The relationship between injected current and instantaneous frequency measured at the1st, 5th and 30th ISI was found to be linear. Note that the upper graph is a representation of the voltage traces illustrated; holding potential, −55 mV. The lower graph constructed from another TC neurone illustrates, by comparison, a much steeper relationship between injected current and instantaneous firing frequency, measured at the 1st ISI; holding potential, − 57 mV. For each current-discharge relationship data were fitted by 1st order regression analysis. The values of injected current are illustrated at the side of the voltage traces. The amplitude of action potentials in *A* and *B* has been truncated for clarity.

interneurones, but not in TC neurones, the time course of the sAHP was truncated and the potential replaced by a slow after-depolarizing potential (sADP) that lasted for up to 15 s following intense firing (Fig. 6*A b*). At the maximum amplitude of the sADP the firing of action potentials (not illustrated) or subthreshold oscillations of the membrane potential were consistently observed (Fig. 6*Aa* and *A b*). In common with the sAHP, the sADP appeared to be related to the number of action potentials generated in the preceding train (Fig. 6*A*). The relative magnitude of the sAHP and sADP was found to vary between interneurones, but in each interneurone examined both potentials were observed. A similar sADP was not observed in TC neurones even following intense action potential firing and so the sADP was considered to be one of the defining electrophysiological features of rat dLGN interneurones.

Burst firing

In each TC neurone examined burst firing was evoked at the break of hyperpolarizing voltage transients. During the construction of voltage–current relationships we measured the instantaneous firing frequency of the burst, at the first ISI, and found it to be linearly related to the amplitude of the preceding voltage deviation, measured at steady state ($r = 0{\cdot}585$, $P < 0{\cdot}05$; Fig. 7*B* and *C*). In each TC neurone

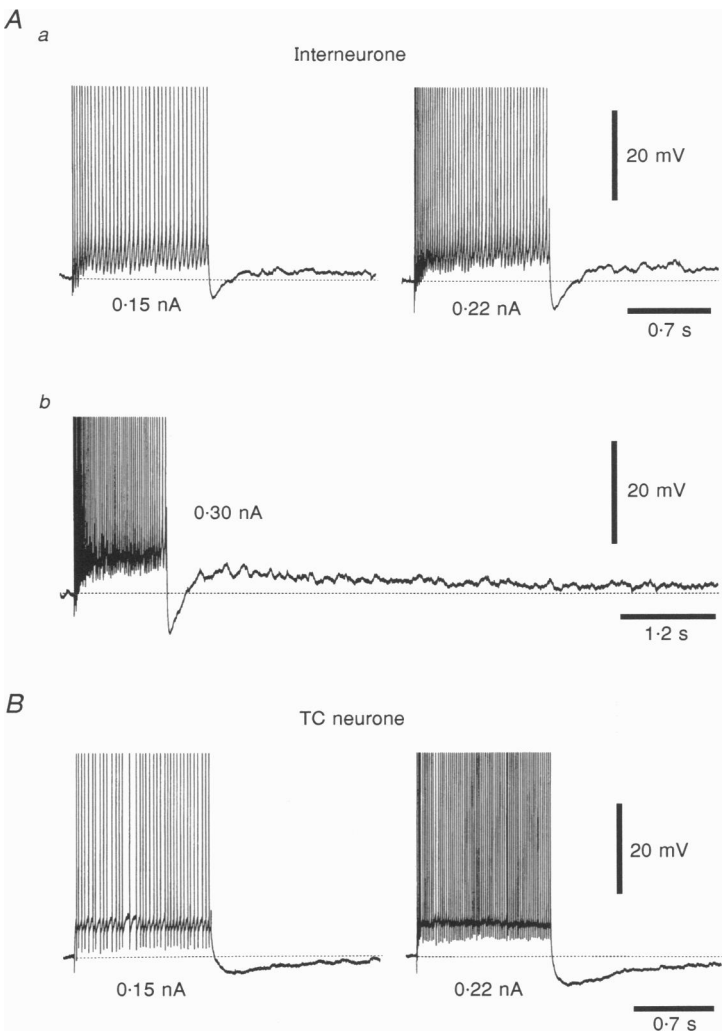

Figure 6. Interneurones but not TC neurones express a post-train slow after-depolarization

A a, following a train of action potentials interneurones were found to generate a slow after-hyperpolarization, the amplitude of which was related to the number of action potentials of the train. This potential was followed by a slow after-depolarization, which increased in amplitude and duration (*A b*) with the increasing number of action potentials of the train. *B*, a representative TC neurone exhibits only a post-train slow after-hyperpolarization, which in common with that of interneurones was related to the number of action potentials of the train. No evidence of a slow after-depolarization was detected. The amplitude of positive current steps is marked below or at the side of the voltage records. The membrane potential at which these activities were evoked was −54 mV for the interneurone and −56 mV for the TC neurone. The amplitude of action potentials has been truncated for clarity.

such activity had a frequency greater than 250 Hz, with a mean frequency of 401 ± 6 Hz. In contrast, the burst firing of interneurones, quantified using the same protocol, was found to be characterized by a lower frequency of action potential output, with a maximal frequency of less than 130 Hz and a mean frequency of 40 ± 5 Hz (Fig. 7*A* and *C*). In common with TC neurones the frequency of rebound firing of interneurones was related in a linear manner to the magnitude of the preceding voltage deviation ($r = 0{\cdot}39$, $P < 0{\cdot}05$) (Fig. 7*C*). In interneurones rebound firing was often characterized by the firing of a single action potential and occasionally it was possible to observe in isolation a transient depolarizing potential that resembled the low threshold Ca^{2+} potential of TC neurones (Fig. 7*A* and *B*). The voltage range over which rebound firing could be evoked at the break of hyperpolarizing voltage excursions was found to be different between groups. Rebound firing could be evoked in interneurones when the holding potential was set at or more positive to −60 mV (Fig. 2), whilst in TC neurones rebound firing could be evoked from membrane potentials more positive than −65 mV (Figs 3 and 5).

Subthreshold oscillation

Membrane potential oscillations were observed in interneurones (Fig. 8). Oscillatory activity was apparent in each interneurone examined, and was expressed over a voltage range positive to −55 mV. The activity had clear periodicity as demonstrated by the autocorrelation analysis of 1 s long segments of voltage traces (Fig. 8, insets). We found the mean frequency of this oscillation for five neurones to be 7·7 ± 0·5 Hz (measured at −44 mV). When the membrane potential of interneurones was depolarized to firing threshold, interneurones, but not TC neurones,

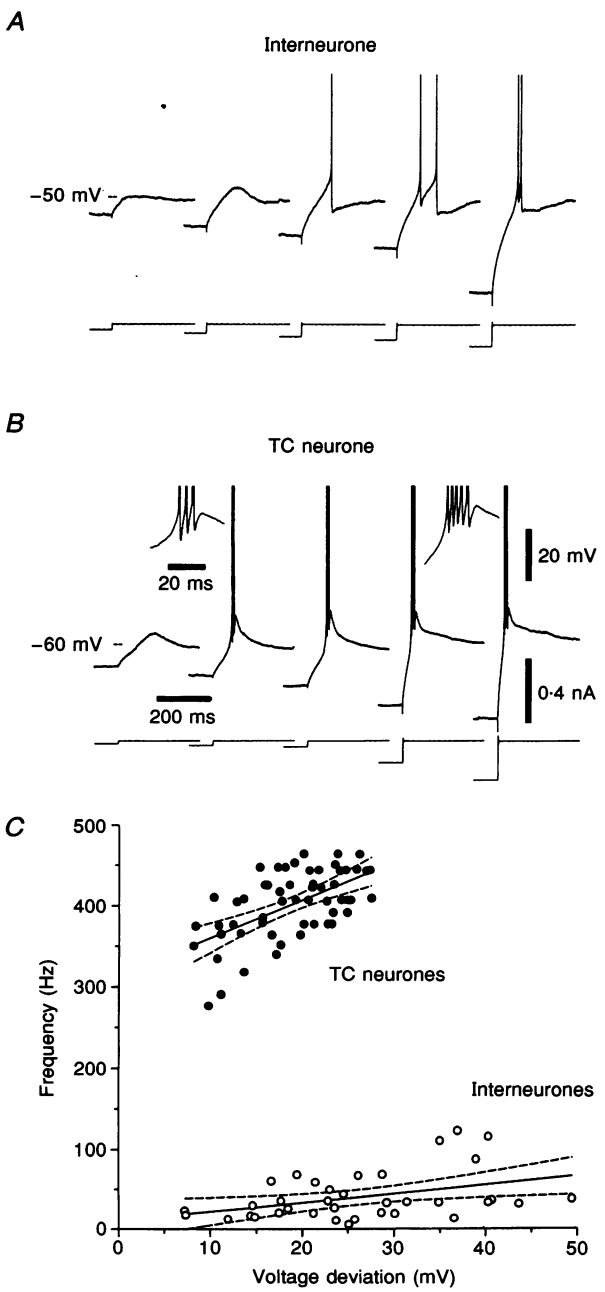

Figure 7. The frequency and structure of rebound burst firing is different between interneurones and TC neurones
At the break of hyperpolarizing voltage deviations, both interneurones and TC neurones generated rebound burst firing. *A*, representative recording of an interneurone demonstrates that the burst firing is driven by a transient depolarizing potential, which gives rise to one or two action potentials. *B*, in comparison the rebound firing of a TC neurone was more powerful: a low threshold Ca^{2+} potential led to the firing of between 3 and 5 action potentials, which are shown as insets at a faster time base. *C*, using the results from a number of such experiments, the frequency of rebound firing (measured as the instantaneous frequency of the first interspike interval) has been plotted against the amplitude of the preceding voltage deviations, measured at steady state for TC neurones (●) and interneurones (○); these measures were found to be linearly related. The data have been fitted by first order regression (continuous line) and the dashed lines indicate the 95% confidence limits. The amplitude of action potentials has been truncated for clarity.

showed an initial period of tonic firing followed by sequences of clustered action potentials intermixed with rhythmic membrane potential oscillations (Fig. 8). This activity profile allowed us to investigate the voltage dependence of the oscillatory activity of interneurones, and indicated that the amplitude and frequency of oscillatory activity, in all cases, increased upon membrane potential depolarization (Fig. 8). The intrinsic nature of oscillatory activity was demonstrated by its resistance to the co-application of the excitatory amino acid (EAA) receptor antagonists GYKI 52466 (100 μM) or CNQX (10 μM) and DL-AP5 (100 μM) (Turner, Leresche, Guyon, Soltesz & Crunelli, 1994). Indeed application of these antagonists increased the periodicity of the oscillation (not illustrated), presumably by removing contaminating activity due to EPSPs and IPSPs that introduced irregularity in the oscillation (see Fig. 11).

Synaptic potentials

EPSPs and IPSPs were evoked in interneurones (Figs 9 and 10) and TC neurones (not illustrated) by electrical stimulation of the optic tract. The nature of the postsynaptic potentials evoked in interneurones was found to be variable; in three of six interneurones apparently pure EPSPs were evoked (Fig. 9). Such potentials had a fast rising phase with a decay that could not be fitted by a mono-exponential function indicating the presence of a slow smaller amplitude component, when EPSPs were evoked from holding potentials positive to −65 mV (Fig. 9).

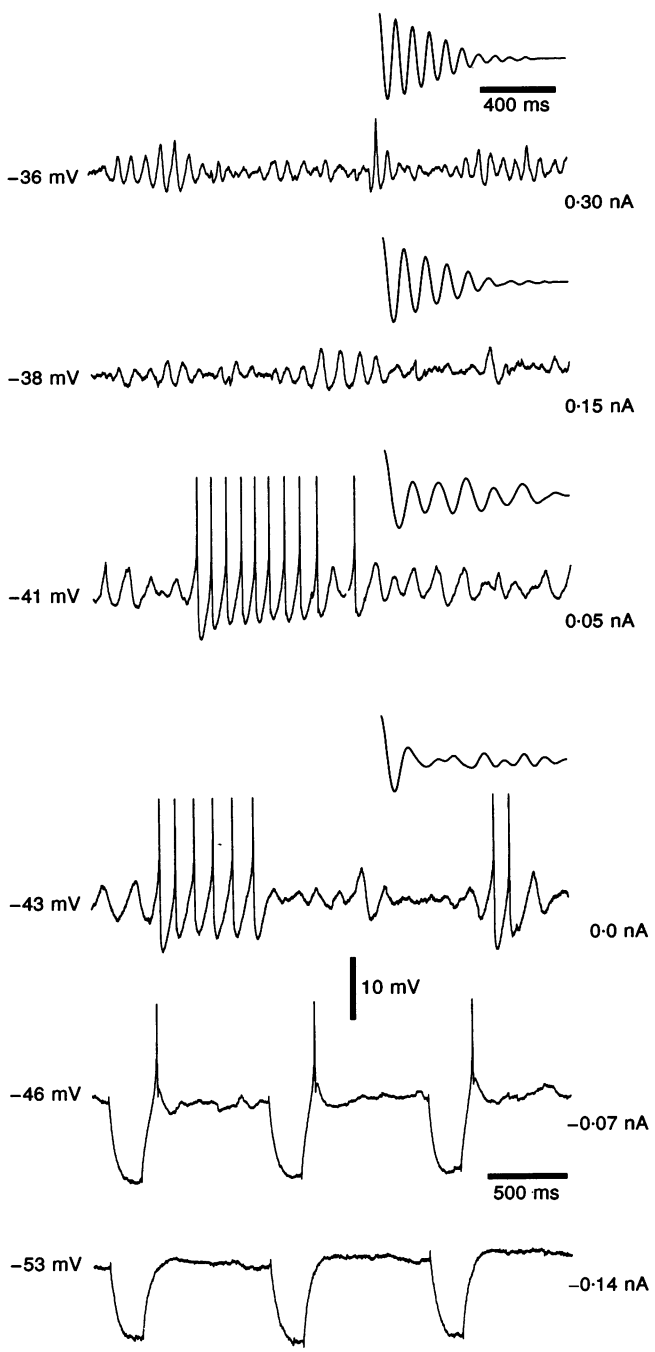

Figure 8. Interneurones exhibit subthreshold oscillatory activity

Interneurones generated subthreshold oscillations within a frequency range of ~8 Hz. The periodicity of this activity is illustrated by the autocorrelation functions (insets above the upper four voltage traces) for 1 s long segments of the voltage trace obtained at different holding potentials. Note that the degree of periodicity increases upon membrane potential depolarization. In the lower two voltage records the hyperpolarizing voltage deviations are generated by the delivery of 0·1 nA square current pulses. Note that near firing threshold a single action potential imposed on a transient depolarizing potential is evoked at the break of hyperpolarizing voltage excursions. The holding potential is shown at the left and magnitude of injected current at the right of voltage traces. The amplitude of action potentials has been truncated for clarity.

When evoked from membrane potentials negative to −65 mV, however, the contribution of the slow component of the EPSPs was found to be reduced (Fig. 9); indeed, in many cases, the decay phase of the fast EPSP component could be well fitted by a mono-exponential function. In each interneurone examined, a single action potential was imposed upon the fast component of the EPSPs when the peak amplitude reached firing threshold (Fig. 9). In contrast, the stimulus-evoked action potential output of TC neurones was more complex; at holding potentials negative to −65 mV EPSPs drove the burst firing of action potentials via the activation of low threshold Ca^{2+} potentials (Deschenes *et al.* 1984; Jahnsen & Llinás, 1984; Turner *et al.* 1994), while at holding potentials positive to −60 mV EPSPs, typically, drove the firing of a single action potential. The differences in the output pattern of interneurones and TC neurones were not due to differing amplitudes of EPSPs (see Turner *et al.* 1994).

Previous investigations of the sensory input to rat and cat TC neurones have indicated the involvement of NMDA and non-NMDA EAA receptors (Scharfman, Lu, Guido, Adams & Sherman, 1990; Leresche, 1992; Turner *et al.* 1994). In interneurones the bath application of the non-NMDA receptor antagonist CNQX (10 μM, $n = 2$) abolished the fast component of the EPSP (Fig. 9*B*). In the presence of CNQX the remaining EPSP had a relatively smaller amplitude and slower time to peak (Fig. 9*B*), and was sensitive to the NMDA receptor antagonist DL-AP5 (100 μM; Fig. 9*C*). Following application of DL-AP5, a low amplitude (<4 mV), slowly rising synaptic potential remained (Fig. 9). Since the pharmacological profile of this potential was not investigated, it remains to be established if this slow EPSP is generated by the activation of other receptors, or if it is a residual product of the lack of full antagonism of NMDA and non-NMDA receptors (see Turner *et al.* 1994).

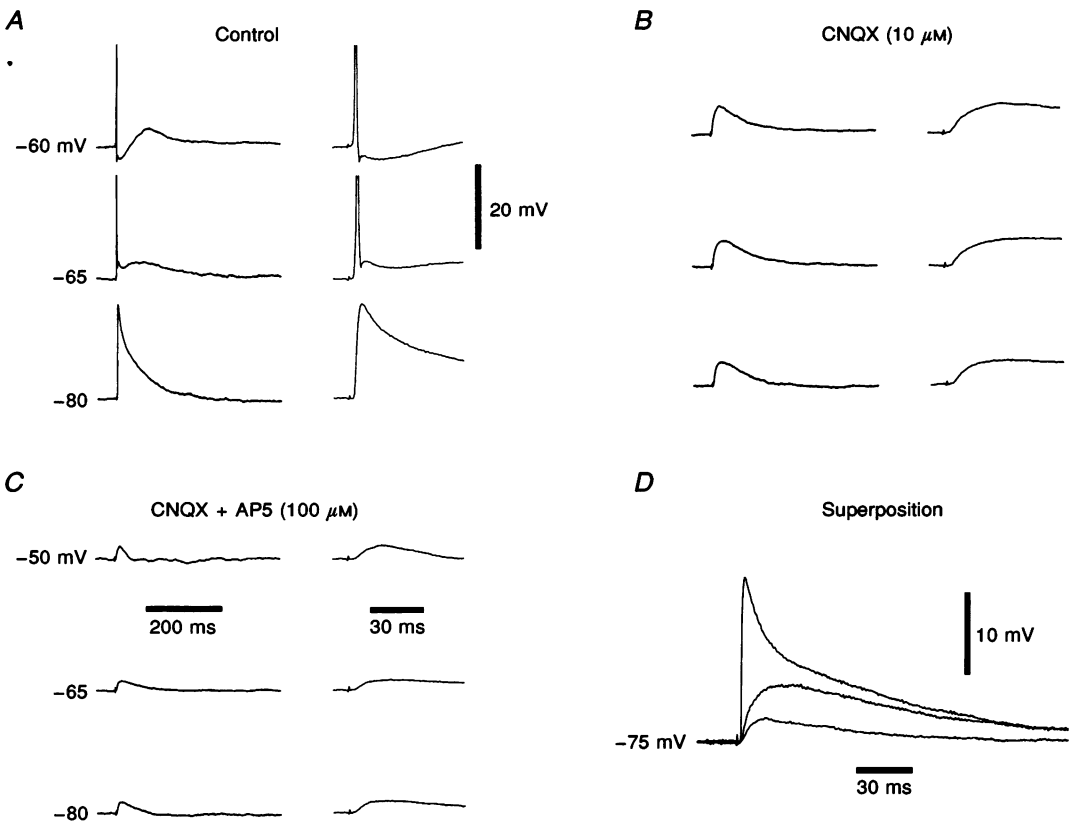

Figure 9. EPSPs of interneurones are mediated by the activation of NMDA and non-NMDA receptors

A, the voltage-dependent profile of control EPSPs evoked by the electrical stimulation of the optic tract is shown at two different time bases. *B*, the bath application of the non-NMDA receptor antagonist CNQX (10 μM) reduced the amplitude of the fast EPSP at all potential levels, leaving a lower amplitude, more slowly rising component that did not reach the threshold for the generation of action potentials. *C*, the additional application of the NMDA receptor antagonist DL-AP5 (100 μM) led to a further decrement in the amplitude of the EPSP leaving a low amplitude (< 4 mV) EPSP with a very slow rise time, which failed to evoke action potentials even when generated at −50 mV. *D*, the superposition of the EPSPs recorded at a level of −75 mV at a fast time base more clearly illustrates the effects of the antagonists. The amplitude of action potentials has been truncated for clarity.

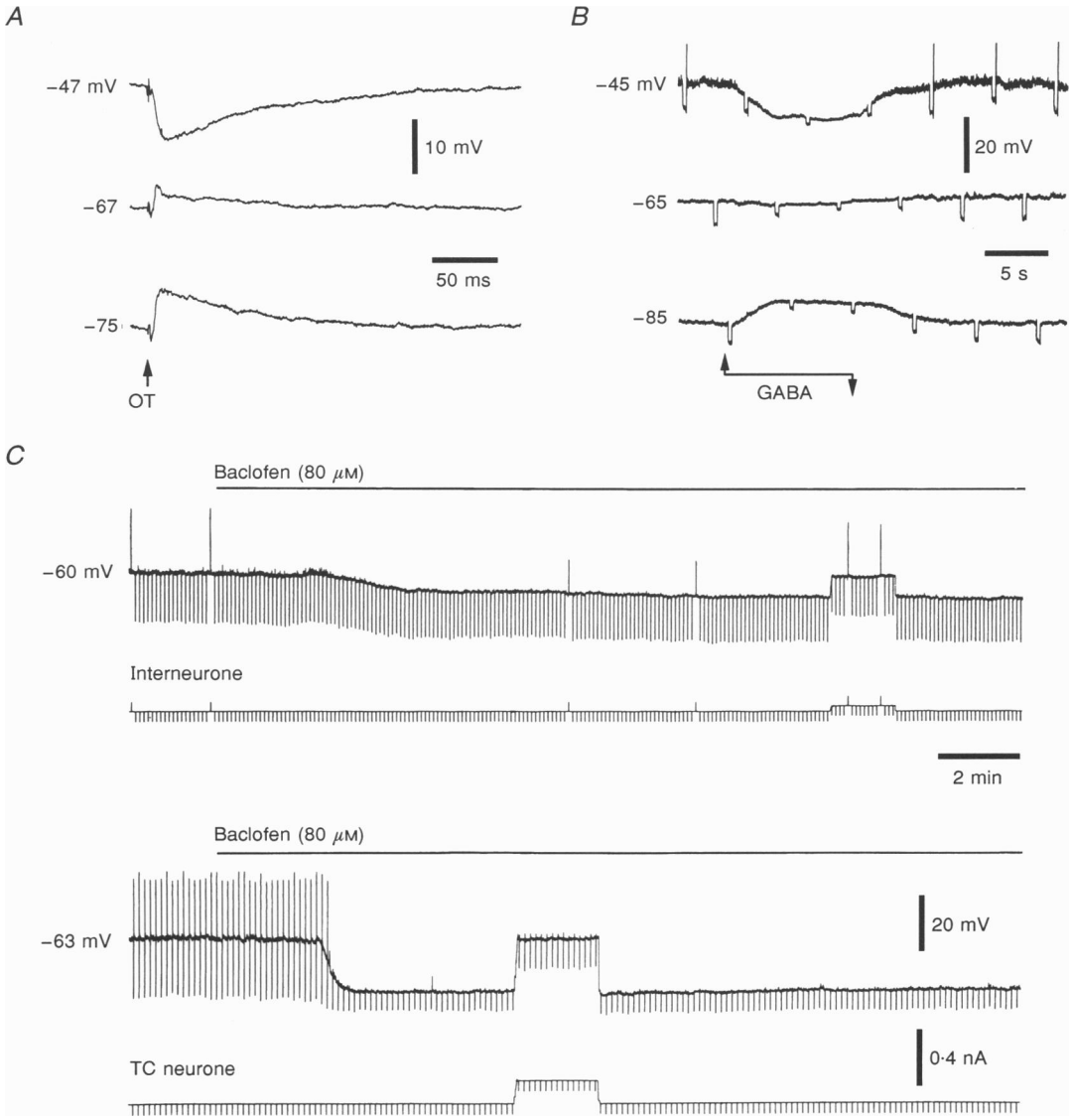

Figure 10. Interneurones are powerfully inhibited by the activation of $GABA_A$, but not $GABA_B$ receptors

A, electrical stimulation of the optic tract evoked an IPSP in this interneurone, which reversed in polarity between −65 and −70 mV. *B*, the iontophoretic application of GABA (70 nA) to the environment of a different interneurone led to a membrane potential hyperpolarization accompanied by a decrease in apparent input resistance: the polarity of this response was found to reverse between −65 and −70 mV. *C*, the bath application of the $GABA_B$ receptor agonist baclofen (80 μM) to this interneurone led to a small membrane potential hyperpolarization accompanied by a decrease in apparent input resistance, which persisted when the membrane potential was set to the control level during the passage of positive current through the recording electrode. Note that this was the only interneurone in which baclofen had any effect. The lower records illustrate the typical effects of baclofen (80 μM) on the membrane properties of a TC neurone recorded from the same brain slice. Note that the magnitude of the baclofen-elicited membrane potential hyperpolarization and decrease in apparent input resistance are greater than those of the interneurone. In the continuous voltage traces downward deflections represent electrotonic potentials evoked by the repeated delivery of constant current pulses. In the recording made from the interneurone, upward deflections represent the firing of action potentials in response to positive current pulses and in the TC neurones upward deflections represent the generation of low threshold Ca^{2+} potentials and action potentials evoked at the break of hyperpolarizing electrotonic potentials. The amplitude of these deflections has been truncated by the frequency response of the chart recorder.

In addition to stimulus-evoked EPSPs, spontaneous EPSPs were recorded from all interneurones (Fig. 2*A*) and in ~30% of TC neurones (not illustrated). The structure of this activity was found to be different between the two groups. In interneurones an almost continuous barrage of spontaneous EPSPs was observed throughout the recording period (Fig. 2*A*), whilst spontaneous EPSPs of TC neurones were observed in clusters, the individual elements of which were often observed to summate. Spontaneous EPSPs were found to be predominantly mediated by the activation of non-NMDA receptors as the application of CNQX (10 μM) greatly reduced the amplitude of these synaptic potentials. The presence of NMDA receptor-mediated spontaneous EPSPs cannot, however, be excluded as the slow rise time and low amplitude of such events could have hampered their detection.

In other interneurones the pattern of stimulus-evoked activity was dominated by inhibition ($n = 3$; Fig. 10*A*). IPSPs were found to reverse in polarity between −65 and −70 mV, in a similar manner to responses to the iontophoretic application of GABA ($n = 2$) to the environment of other interneurones (Fig. 10*B*). The potency of the inhibition produced by either electrical stimulation or iontophoretic application of GABA was demonstrated by the silencing of on-going action potential firing (not illustrated). In order to compare the differential effects of the activation of $GABA_A$ and $GABA_B$ receptors, we applied by bath perfusion the selective $GABA_B$ receptor agonists baclofen (at concentrations up to 100 μM; $n = 4$; Crunelli *et al.* 1988) and γ-hydroxybutyrate (GHB; 1–3 mM; $n = 3$; Williams, Turner & Crunelli, 1995*b*). In the majority of interneurones these agonists had no effect on either the membrane potential or apparent input resistance. However, in one interneurone (Fig. 10*C*) the application of baclofen (80 μM) led to a small membrane potential hyperpolarization (7 mV) and decrease in apparent input resistance. This effect was, however, relatively weak in comparison with the effects of the same concentration of baclofen on the membrane potential and apparent input resistance of a TC neurone recorded from the same preparation (Fig. 10*C*).

Spontaneously occurring IPSPs were recorded from interneurones (Fig. 11) and TC neurones (not illustrated). These IPSPs were found to be intermixed with spontaneous EPSPs and subthresold oscillatory activity of interneurones, but they could be clearly identified by their reversal potential of between −65 and −70 mV (Fig. 11). The presence of spontaneous IPSPs suggests that interneurones are subject to a tonic level of inhibition when maintained in brain slices *in vitro*. The similar reversal potential of spontaneous and stimulus-evoked IPSPs suggests the activation of a common type of receptor.

DISCUSSION

The main conclusions of this investigation are that (i) two populations of neurones, termed interneurones and TC neurones, with distinct electroresponsiveness and morphological properties, can be distinguished in the rat dLGN; (ii) interneurones possess characteristic electrophysiological features that include the shape of single action potentials and their fAHP, the presence of a slow and pronounced spike-frequency adaptation, the presence of post-train sADPs, the generation of subthreshold oscillatory activity with a frequency of ~8 Hz, the low frequency firing at the

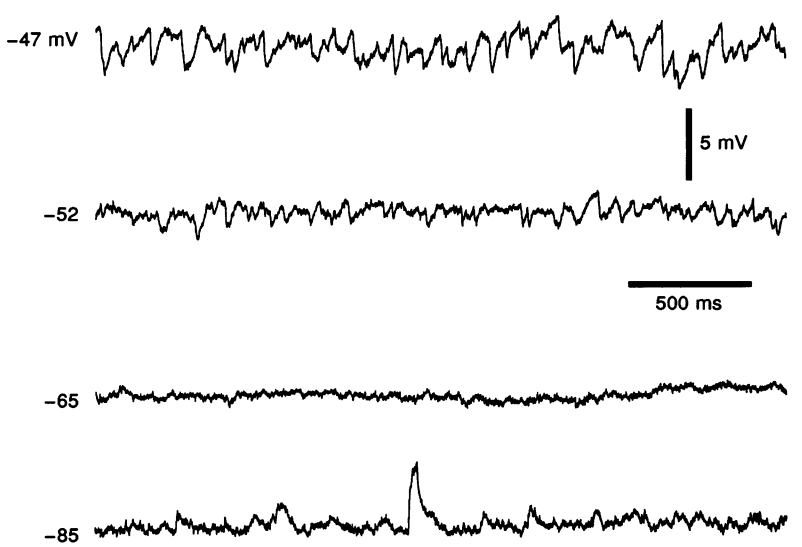

Figure 11. Interneurones are subject to tonic inhibition

Spontaneous IPSPs were recorded from an interneurone at different holding potentials, achieved by the tonic passage of current though the recording electrode (−47 mV is the resting potential). The IPSPs appear to reverse in polarity at holding potentials between −65 and −70 mV. In the upper voltage record IPSPs are intermixed with the intrinsic subthreshold oscillatory activity of this interneurone; in the lower records the individual IPSPs are distinguishable.

break of hyperpolarizing voltage excursions and the nearly linear nature of voltage–current relationships; and (iii) there are interneurone to interneurone inhibitory interactions in the rat dLGN.

Comparative anatomical properties

By comparison with the results of Golgi impregnation (Grossman *et al.* 1973; Gabbot *et al.* 1986) and HRP injection studies (Crunelli *et al.* 1987), the morphology of biocytin-injected neurones was classified as class A (TC neurones) and class B (putative interneurones). The dorsoventral dendritic orientation of interneurones and the radial fields of TC neurones are in accordance with previous studies and may contribute to the their respective rectangular and circular receptive field properties (Fukuda, Sumitomo, Sugitani & Iwama, 1979). In the present study the recording of neurones of different morphologies and electrophysiological responsiveness in single brain slices clearly indicates a heterogeneous population of neurones in the rat dLGN. Although we encountered subtle morphological differences between neurones classified as belonging to the same group we have found no evidence for a finer classification system of TC neurones.

Comparative electrophysiological properties

Passive properties

The passive membrane properties of interneurones and TC neurones were found to be different. The resting potentials of interneurones were significantly more positive and the time constants shorter than those of TC neurones. As the same methods, and occasionally the same electrode, were used to record interneurones and TC neurones a comparison between neuronal type should be valid. A degree of caution should, however, be considered when interpreting these data, as the influence of background synaptic activity (Bernander, Douglas, Martin & Koch, 1991) and the degree of neuronal damage, and so the generation of a somal shunt (Staley, Otis & Mody, 1992), are thought to affect such measurements. Indeed these points are important as interneurones were found to have smaller somal areas and a greater degree of spontaneous synaptic activity than TC neurones.

Rectification properties

The rectification properties of interneurones were found to be distinct from those of TC neurones: voltage–current relationships of interneurones lacked the prominent rectification properties of TC neurones that are expressed in both the depolarized and hyperpolarized direction. The rectifiation of the voltage–current relationship of TC neurones in the depolarized direction is thought to be mediated by slowly inactivating K^+ currents (Huguenard & Prince, 1991). These slowly inactivating K^+ currents in concert with a more transient I_A-like current act to delay the onset of action potential firing (Huguenard & Prince, 1991). The lack of a substantial delay to firing in interneurones and the absence of rectification in the depolarized direction suggests a minimal expresson of these currents. However, the brief delay to firing in interneurones, when action potentials were evoked from holding potentials negative to −60 mV, is indicative of the presence of fast transient outward K^+ currents, e.g. I_A. These data suggest that interneurones should fire briskly in response to afferent activity, as indicated by recordings of identified cat dLGN interneurones *in vivo* (Humphrey & Weller, 1988). The rectification of the voltage–current relationship of TC neurones in the hyperpolarized direction is thought to be generated by the activation of a slow, mixed cation current, I_h (McCormick & Pape, 1990) and a fast K^+-mediated current (Pollard & Crunelli, 1988). A similar slow rectification was expressed in some interneurones; although the magnitude of such rectification was not as great as that of TC neurones, this parameter cannot be used to classify neuronal type. In addition to time-dependent rectification we observed the presence of steady rectification of interneurones, which led to a greater apparent input resistance at potentials close to firing threshold. These data indicate that although interneurones have nearly linear voltage–current relationships the effects of excitatory and inhibitory inputs will be greater at subthreshold membrane potentials.

Burst firing

At the break of hyperpolarizing voltage excursions, interneurones and TC neurones were found to generate a transient depolarizing potential that was crowned by the firing of action potentials; the frequency of such firing was, however, significantly slower in interneurones. The voltage range over which such activity could be generated was also different between groups, suggesting that the voltage-dependence of the current(s) that underlie(s) the transient depolarizing potentials are different. Previous analysis has indicated that the transient depolarizing potentials of TC neurones are generated by a low threshold Ca^{2+} current, I_T, that is available for activation at potentials negative to ~−65 mV (Crunelli *et al.* 1989). A recent investigation has revealed that interneurones, dissociated from the rat dLGN, also express an I_T-like current. The steady-state activation and inactivation curves of this current were, however, found to be shifted by ~10 mV positive to that of TC neurones (Pape *et al.* 1994). Such a difference in the voltage dependence of I_T between neurones may explain the different voltage range over which we observed transient depolarizing potentials and burst firing between neuronal type. In dissociated interneurones the expression of I_T in current clamp recordings was found to be masked by the activation of an I_A-like current (Pape *et al.* 1994). It is not clear to what extent such a mechanism operates in interneurones maintained in more intact preparations, as rebound firing has been observed from recordings of putative thalamic interneurones of the guinea-pig (Jahnsen & Llinás, 1984) and morphologically identified interneurones of the cat dLGN (McCormick & Pape, 1988). The measurement of I_T and I_A and an analysis of the effects of pharmacological blockade of I_A are therefore required for a full interpretation of this behaviour.

Subthreshold oscillations

Interneurones were found to express intrinsic (~8 Hz), subthreshold membrane potential oscillatory activity. These activities did not resemble the well-characterized low frequency (<4 Hz; McCormick & Pape, 1990; Leresche *et al.* 1991; Steriade, Curro Dossi & Nunez, 1991; Williams *et al.* 1995*b*) and high frequency (>20 Hz; Steriade, Curro Dossi, Pare & Oakson, 1991) oscillatory activities of TC neurones, but were similar to the subthreshold oscillatory activity expressed by cortical stellate neurones (Klink & Alonso, 1993). The ionic basis of the oscillatory activity of cortical stellate neurones has been shown to be mediated by the activation of a persistent Na^+ current and a K^+ current activated at subthreshold membrane potentials (Klink & Alonso, 1993). Although we did not investigate the ionic basis of the oscillatory activity of interneurones, the similarity in the electrophysiological behaviour of thalamic interneurones and cortical stellate neurones, in terms of their rectification properties, discharge patterns and in particular the presence of a slow depolarizing ramp pre-potential preceding the fast upstroke of the single action potentials, suggests that the oscillatory activity of dLGN interneurones may be generated by a similar set of membrane currents as those of stellate neurones. We cannot, however, rule out the possibility that the sub-threshold oscillatory activity of interneurones is mediated by a different mechanism involving, for example, the activation of low and high threshold Ca^{2+} currents.

The membrane potential oscillatory activity of inter-neurones may drive a similar frequency of action potential output, leading to the generation of IPSPs in interneurones and TC neurones. In our preparations we recorded spontaneous IPSPs from interneurones and TC neurones. Previous investigations of TC neurones recorded *in vitro* (Leresche, 1992) and *in vivo* (Steriade, Deschenes, Domich & Mulle, 1985) have reported spontaneous IPSPs; indeed *in vivo* the frequency of spontaneous IPSPs was found to be centred at ~10 Hz, when the main thalamic nuclei were functionally disconnected from the NRT (Steriade *et al.* 1985). The function of the oscillatory activity of interneurones may be to drive an output of TC neurones within a similar frequency range. Such an interpretation has been made for the control of the output of pyramidal neurones of the hippocampus, where spontaneous IPSPs, occurring within the frequency range of 40 Hz, have been shown to drive the output of pyramidal neurones within a similar frequency range (Whittington, Traub & Jefferys, 1995). The results of field recordings made from the dLGN of unanaesthetized cats, have indicated the presence of oscillatory activity with a frequency of ~10 Hz (Chatila, Milleret, Rougeul & Buser, 1993). The similarity between this frequency and the frequency of subthreshold activity of dLGN interneurones suggests that intereurones may be involved in the synchronization of such a rhythm.

Action potential firing pattern

Interneurones, but not TC neurones, demonstrated discharge patterns marked by a slow and pronounced spike-frequency adaptation. Previous findings have indicated the discharge pattern of interneurones of the cat dLGN recorded *in vitro* and *in vivo* to be dominated by spike-frequency adaptation (Humphrey & Weller, 1988; McCormick & Pape, 1988). Cat dLGN interneurones, in contrast to those recorded here, were, however, found to discharge at very high frequencies (McCormick, Pape, Kisvardy & Eysel, 1992). The discharge pattern of rat and cat dLGN interneurones may, therefore, be different in terms of peak firing frequency, but not in the structure of discharge patterns. These data indicate that from holding potentials positive to −60 mV the output of interneurones and TC neurones will be similar to transient afferent inputs but become progressively dissimilar to more sustained inputs. We suggest that the spike-frequency adaptation of interneurones contributes to the formation of the lagged responses (Humphrey & Weller, 1988; Heggelund & Hartveit 1990) of some dLGN TC neurones. The lag period is known to be formed, in the majority, by $GABA_A$ receptor-mediated inhibition (Heggelund & Hartveit, 1990) and is thought to involve intra-geniculate circuits, but not inputs from the PGN (Humphrey & Weller, 1988). As the interneurones reported here were found to be driven by the activation of non-NMDA and NMDA receptors, to have a fast onset to action potential firing and to display prominent spike-frequency adaptation, it is possible that through the course of a retinal input the rate of firing decreases, leading to a reduction in the temporal summation of IPSPs (generated by the axonal output of interneurones) in postsynaptic TC neurones. This mechanism may create a greater degree of inhibition at the onset of retinal input that is relatively amplified in lagged TC neurones, as the input to these units is known to be mediated, preferentially, by the activation of NMDA receptors (Heggelund & Hartveit, 1990). Factors such as the voltage dependence and the rise and decay times of NMDA receptor-mediated EPSPs may be critical in the differential effects of inhibition in lagged and non-lagged neurones (Heggelund & Hartveit, 1990).

Following a train of action potentials both interneurones and TC neurones generated a sAHP; the time course of the sAHP in interneurones was, however, truncated and the potential replaced by a sADP, which in many cases had action potentials and/or subthreshold oscillations imposed upon it. This sADP may function to maintain the discharge of interneurones following the termination of afferent input, and by the generation of postsynaptic inhibition of TC neurones add to the effects of the sAHP in these neurones. These mechanisms may contribute to the limitation of following frequency of TC neurones. It is, therefore, of interest that blockade of $GABA_A$ receptor-mediated inhibition leads to an increased output of X-type TC neurones in response to stimuli of increasing temporal frequency (Berardi & Morrone, 1984).

Excitation and inhibition of interneurones

EPSPs and IPSPs were generated in interneurones by low frequency electrical stimulation of the optic tract; the contribution made by EPSPs and IPSPs to the complex synaptic response was found to be variable, as reported for TC neurones (Crunelli *et al.* 1988). EPSPs generated in interneurones were found to be bi-phasic and mediated by the activation of non-NMDA and NMDA receptors, as has been shown for EPSPs and excitatory postsynaptic currents evoked in TC neurones (Scharfman *et al.* 1990; Leresche, 1992; Turner *et al.* 1994). The pharmacological profile of stimulus-evoked IPSPs was not directly investigated, but we suggest that inhibition is mediated predominantly by the activation of $GABA_A$ receptors since (i) IPSPs and the responses to the iontophoretic application of GABA were found to reverse at membrane potentials between −65 and −70 mV, (ii) the rise time, duration and reversal potential of IPSPs in interneurones were found to be similar to $GABA_A$ receptor-mediated IPSPs evoked in rat dLGN TC neurones by optic tract stimulation (Crunelli *et al.* 1988), and (iii) the bath application of the $GABA_B$ receptor agonists were, with the exception of one neurone, found to have no effects on the membrane potential or apparent input resistance of interneurones. The absence of $GABA_B$ receptor-mediated IPSPs and the low sensitivity to selective $GABA_B$ agonists is in contrast to that of TC neurones (Crunelli *et al.* 1988; Soltesz *et al.* 1989; Williams *et al.* 1995*b*), and suggest that interneurones express a relatively low number of $GABA_B$ receptors.

These data demonstrate that stimulation of the optic tract may reliably bring interneurones to firing threshold, and so indicate that feed-forward IPSPs evoked in TC neurones are generated at least in part through the axonal output of dLGN interneurones. We cannot, however, exclude the possibility that feed-forward IPSPs evoked in TC neurones are mediated, in part, by the dendritic elements of interneurones that are known to enter into and form a triadic arrangement with optic tract terminals and TC neurone dendrites (Grossman *et al.* 1973; Hamos *et al.* 1985). Our observations that interneurones are also subject to stimulus-evoked inhibition indicate that the activities of interneurones are controlled by inhibitory influences. The cellular origin of this inhibition may be from fellow interneurones of the dLGN, as brain slices were prepared in a manner that excluded the NRT and so the pathway underlying feed-back inhibition (Hale *et al.* 1982; Lindstrom, 1982). Whilst it is possible that IPSPs were generated by the direct depolarization of the axons of NRT neurones, the low voltage of electrical stimuli and the position of stimulating electrodes in the most lateral margin of the optic tract suggests that current spread to the axons of NRT neurones is unlikely. We therefore, suggest that evoked IPSPs were generated by other dLGN interneurones. In addition to stimulus-evoked inhibition, interneurones were subject to spontaneous IPSPs. The source of spontaneous IPSPs cannot be critically analysed, and so they may be generated by the activities of other interneurones, or axons of NRT neurones. No anatomical or electrophysiological evidence gained from the rat visual thalamus is available to describes a pathway from the NRT to dLGN interneurones. In the cat unequivocal anatomical evidence for the existence of such pathway is also lacking (Cucchiaro, Uhlrich & Sherman, 1992), but electrophysiological evidence suggests such a pathway exists (Ahlsen, Lindstrom & Lo, 1985). The site(s) of origin of spontaneous IPSPs cannot fully be described until further investigations are conducted.

The functional consequences of the inhibition of interneurones are difficult to interpret. Previous investigations, however, have demonstrated that the magnitude of stimulus-evoked $GABA_B$ receptor-mediated IPSPs may be enhanced following the antagonism of $GABA_A$ receptors (Crunelli *et al.* 1988; Soltesz *et al.* 1989). One interpretation of these effects is that an antagonism of the $GABA_A$ receptor-mediated inhibition of interneurones leads to an increased action potential output of these neurones (Crunelli *et al.* 1988; Soltesz *et al.* 1989). The presence of interneurones that receive stimulus-evoked excitation and $GABA_A$ receptor-mediated inhibition provide evidence in favour of such a hypothesis. However, as we have not tested the effects of $GABA_A$ receptor antagonists on the evoked activity of interneurones we may only speculate that the action potential output of these neurones would be increased by the antagonism of $GABA_A$ receptors. Nevertheless, the present data suggest that the nature of the inhibition of TC neurones of the dLGN is dependent upon the network properties of the nucleus. The nature of inhibition of TC neurones and the mechanisms by which the inhibition of interneurones is removed physiologically may be of importance to the function of the dLGN.

Ahlsen, G. & Lindstrom, S. (1982). Excitation of perigeniculate neurones via axon collaterals of principle cells. *Brain Research* **236**, 477–481.

Ahlsen, G., Lindstrom, S. & Lo, F. S. (1985). Interaction between inhibitory pathways to principle cells in the lateral geniculate nucleus of the cat. *Experimental Brain Research* **58**, 134–143.

Berardi, N. & Morrone, M. C. (1984). The role of gamma-amino-butyric acid mediated inhibition in the response properties of cat lateral geniculate nucleus neurones. *Journal of Physiology* **377**, 505–523.

Bernander, O., Douglas, R. J., Martin, K. A. C. & Koch, C. (1991). Synaptic background activity influences spatiotemporal integration in single pyramidal cells. *Proceedings of the National Academy of Sciences of the USA* **88**, 11569–11573.

Chatila, M., Milleret, C., Rougeul, A. & Buser, P. (1993). Alpha rhythm in the cat thalamus. *Comptes Rendus de l'Academie des Sciences*, série III, *Science de la Vie* **316**, 51–58.

Crunelli, V., Kelly, J. S., Leresche, N. & Pirchio, M. (1987). The ventral and dorsal lateral geniculate nucleus of the rat: intracellular recordings *in vitro*. *Journal of Physiology* **384**, 587–601.

CRUNELLI, V., HABY, M., JASSIK-GERSCHENFELD, D., LERESCHE, N. & PIRCHIO, M. (1988). Cl^- and K^+ -dependent inhibitory postsynaptic potentials evoked by interneurones of the rat lateral geniculate nucleus. *Journal of Physiology* **399**, 153–176.

CRUNELLI, V., LIGHTOWLER, S. & POLLARD, C. E. (1989). A T-type Ca^{2+} current underlies low-threshold Ca^{2+} potentials in cells of the cat and rat lateral geniculate nucleus. *Journal of Physiology* **413**, 543–561.

CUCCHIARO, J. B., UHLRICH, D. J. & SHERMAN, S. M. (1991). Electron-microscopic analysis of synaptic input from the perigeniculate nucleus to the A-laminae of the lateral geniculate nucleus in cats. *Journal of Comparative Neurology* **319**, 316–336.

DESCHENES, M., PARADIS, M., ROY, J. P. & STERIADE, M. (1984). Electrophysiology of neurons of lateral thalamic nuclei in cat: resting properties and burst discharges. *Journal of Neurophysiology* **51**, 1196–1219.

FUKUDA, Y., SUMITOMO, I., SUGITANI, M. & IWAMA, K. (1979). Receptive-field properties of cells in the dorsal part of the albino rat's lateral geniculate nucleus. *Japanese Journal of Physiology* **29**, 283–307.

GABBOT, P. L. A., SOMOGYI, J., STEWART, M. G. & HAMORI, J. (1986). GABA-immunoreactive neurons in the dorsal lateral geniculate nucleus of the rat: characterisation by combined Golgi-impregnation and immunocytochemistry. *Experimental Brain Research* **61**, 311–322.

GROSSMAN, A., LIBERMAN, A. R. & WEBSTER, K. E. (1973). A Golgi study of the rat lateral geniculate nucleus. *Journal of Comparative Neurology* **150**, 441–446.

HALE, P. T., SEFTON, A. J., BAUR, L. A. & COTTEE, L. J. (1982). Interrelations of the rat's thalamic reticular and dorsal lateral geniculate nuclei. *Experimental Brain Research* **45**, 217–229.

HAMOS, J. E., VAN HORN, S. C., RACZKOWSKI, D., UHLRICH, D. J. & SHERMAN, S. M. (1985). Synaptic connectivity of a local circuit neurone in lateral geniculate nucleus of the cat. *Nature* **317**, 618–621.

HEGGELUND, P. & HARTVEIT, E. (1990). Neurotransmitter receptors mediating excitatory input to cells in the cat lateral geniculate nucleus. I. Lagged cells. *Journal of Neurophysiology* **63**, 1347–1372.

HUGUENARD, J. R. & PRINCE, D. A. (1991). Slow inactivation of a TEA-sensitive K current in acutely isolated rat thalamic neurons. *Journal of Neurophysiology* **66**, 1316–1328.

HUMPHREY, A. L. & WELLER, R. E. (1988). Structural correlates of functionally distinct X-cells in the lateral geniculate nucleus of the cat. *Journal of Comparative Neurology* **268**, 448–468.

JAHNSEN, H. & LLINÁS R. (1984). Electrophysiological properties of guinea-pig thalamic neurones: an *in vitro* study. *Journal of Physiology* **349**, 205–226.

JONES, H. E. & SILLITO, A. M. (1994). Responses of cells in the dorsal lateral geniculate nucleus (LGN) during inactivation of the perigeniculate nucleus. *Neuroscience Abstracts* **20**, 61.12.

KLINK, R. & ALONSO, A. (1993). Ionic mechanisms for the subthreshold oscillations and differential electroresponsiveness of medial entorhinal cortex layer II neurons. *Journal of Neurophysiology* **70**, 144–157.

LERESCHE, N. (1992). Synaptic currents in thalamo-cortical neurons of the rat lateral geniculate nucleus. *European Journal of Neuroscience* **4**, 595–602.

LERESCHE, N., LIGHTOWLER, S., SOLTESZ, I., JASSIK-GERSCHENFELD, D. & CRUNELLI, V. (1991). Low-frequency oscillatory activities intrinsic to rat and cat thalamocortical cells. *Journal of Physiology* **441**, 155–174.

LINDSTROM, S. (1982). Synaptic organization of inhibitory pathways to principle cells in the lateral geniculate nucleus of the cat. *Brain Research* **234**, 447–453.

MCCORMICK, D. A. & PAPE, H.-C. (1988). Acetylcholine inhibits identified interneurons in the cat lateral geniculate nucleus. *Nature* **334**, 246–248.

MCCORMICK, D. A. & PAPE, H.-C. (1990). Properties of a hyperpolarization-activated cation current and its role in rhythmic oscillations in thalamic relay neurones. *Journal of Physiology* **431**, 291–342.

MCCORMICK, D. A., PAPE, H.-C., KISVARDY, Z. & EYSEL, U. T. (1992). Electrophysiological and pharmacological properties of LGNd interneurons. *Neuroscience Abstracts* **18**, 101.1.

MONTERO, V. M. (1987). Ultrastructural identification of synaptic terminals from the axon of type 3 interneurons in the cat lateral geniculate nucleus. *Journal of Comparative Neurology* **264**, 268–283.

NORTON, T. T. & GODWIN, D. W. (1992). Inhibitory GABAergic control of visual signals at the lateral geniculate nucleus. *Progress in Brain Research* **90**, 193–217.

PAPE, H. C., BUDDE, T., MAGER, R. & KISVARDAY, Z. F. (1994). Prevention of Ca^{2+}-mediated action potentials in GABAergic local circuit neurones of rat thalamus by a transient K^+ current. *Journal of Physiology* **478**, 403–422.

POLLARD, C. E. & CRUNELLI, V. (1988). Intrinsic membrane currents in projection cells of the cat and rat lateral geniculate nucleus. *Neuroscience Letters* **S32**, 29.

OHARA, P. T., LIBERMAN, A. R., HUNT, S. P. & WU, J.-Y. (1983). Neural elements containing glutamic acid decarboxylase (GAD) in the dorsal lateral geniculate nucleus of the rat: immunohistochemical studies by light and electron microscopy. *Neuroscience* **8**, 189–211.

SCHARFMAN, H. E., LU, S.-M., GUIDO, W., ADAMS, P. R. & SHERMAN, S. M. (1990). N-methyl-D-aspartate (NMDA) receptors contribute to EPSPs of cat lateral geniculate neurons recorded in thalamic slices. *Proceedings of the National Academy of Sciences of the USA* **87**, 4548–4552.

SILLITO, A. M. & KEMP, J. A. (1983). The influence of GABAergic inhibitory processes on the receptive field structure of X and Y cells in the cat dorsal lateral geniculate nucleus (dLGN). *Brain Research* **277**, 63–77.

SOLTESZ, I., LIGHTOWLER, S., LERESCHE, N. & CRUNELLI, V. (1989). On the properties and origin of the $GABA_B$ inhibitory postsynaptic potential recorded in morphologically identified projection cells of the cat dorsal lateral geniculate nucleus. *Neuroscience* **33**, 23–33.

SPREAFICO, R., SCHMECHEL, D. E. & RUSTIONI, A. (1983). Cortical relay neurones and interneurones in the N. ventralis posterolateralis of cats: a horseradish peroxidase, electron-microscope, Golgi and immunocytochemical study. *Journal of Neuroscience* **9**, 491–509.

STALEY, K. J., OTIS, T. S. & MODY, I. (1992). Membrane properties of dentate gyrus granule cells – comparison of sharp microelectrodes and whole-cell recordings. *Journal of Neurophysiology* **67**, 1346–1358.

STERIADE, M., CURRO DOSSI, R., PARE, D. & OAKSON, G. (1991). Fast oscillations (20–40 Hz) in thalamocortical systems and their potentiation by mesopontine chloinergic nuclei in the cat. *Proceedings of the National Academy of Sciences of the USA* **88**, 4396–4400.

STERIADE, M., CURRO DOSSI, R. & NUNEZ, A. (1991). Network modulation of a slow intrinsic oscillation of cat thalamocortical neurons implicated in sleep delta waves: cortical induced synchronization and brainstem cholinergic suppression. *Journal of Neuroscience* **11**, 3200–3217.

STERIADE, M., DESCHENES, M., DOMICH, L. & MULLE, C. (1985). Abolition of spindle oscillations in thalamic neurons disconnected from nucleus reticularis thalami. *Journal of Neurophysiology* **54**, 1473–1497.

TURNER, J. P., LERESCHE, N., GUYON, A., SOLTESZ, I. & CRUNELLI, V. (1994). Sensory input and burst firing output of rat and cat thalamocortical cells: the role of NMDA and non-NMDA receptors. *Journal of Physiology* **480**, 281–295.

WHITTINGTON, M. A., TRAUB, R. D. & JEFFERYS, J. G. R. (1995). Synchronized oscillations in interneuron networks driven by metabotropic glutamate receptor activation. *Nature* **373**, 612–615.

WILLIAMS, S. R., ANDERSON, C. M. & CRUNELLI, V. (1995*a*). Electrophysiological and morphological properties of local circuit interneurones of the rat dorsal lateral geniculate nucleus *in vitro*. *Journal of Physiology* **483.P**, 58*P*.

WILLIAMS, S. R., TURNER, J. P. & CRUNELLI, V. (1994). Pharmacological and electrophysiological properties of local circuit interneurones in brain slices of the rat dorsal lateral geniculate nucleus. *Neuroscience Abstracts* **20**, 10.9.

WILLIAMS, S. R., TURNER, J. P. & CRUNELLI, V. (1995*b*). Gamma-hydroxybutyrate promotes oscillatory activity of rat and cat thalamocortical neurons by a tonic $GABA_B$ receptor-mediated hyperpolarization. *Neuroscience* **66**, 133–143.

Acknowledgements

We would like to thank Mr Tim Gould for help with anatomical recovery and the manufacture of iontophoresis electrodes, Mr Bob Jones for photography, Dr Andy Schering for his advice on anatomical techniques and Dr Pedro Lowenstein for the use of equipment. The support of the Wellcome Trust (grant 37089) is gratefully acknowledged. S.R.W. was supported by a Wellcome Prize Studentship.

Received 17 March 1995; accepted 5 July 1995.